



FLOW INVESTIGATIONS IN ACHARD TURBINE

Sandor BERNAD*, Andrei GEORGESCU**, Sanda-Carmen GEORGESCU***, Romeo SUSAN-RESIGA****, Ioan ANTON****

*Centre of Advanced Research in Engineering Sciences, Romanian Academy, Timisoara Branch, 300223, Timisoara

**Department of Hydraulics and Environmental Protection, Technical Civil Engineering University Bucharest, RO-020396
Bucharest, Romania

***Department of Hydraulics and Hydraulic Machinery, "Politehnica" University of Bucharest, RO-060042, Bucharest, Romania

****Department of Hydraulic Machinery, "Politehnica" University of Timisoara, RO-300222, Timisoara, Romania

Corresponding author: Sandor Bernad, Romanian Academy – Timisoara Branch,

Bd. Mihai Viteazul 24, 300223 Timisoara, phone: +40 256 403692, fax: +40 256 403700, email: sbernad@mh.mec.upt.ro

Tidal current generation uses a generator to produce energy, changing the kinetic energy of current into a turning force by setting a water turbine in the tidal current. Therefore, it is considered to be very advantageous to use a water turbine that can always revolve in a fixed direction without any influence from tidal current directions. Water turbines with these characteristics are known as Darrieus water turbines. In this paper we investigated the new type of concept of water-current turbine, called *Achard turbine*. Two-dimensional numerical modelling of the unsteady flow through the blades of the Achard turbine, is performed using Fluent 6.3 software.

Key words: marine turbine, Achard turbine, numerical simulation

NOMENCLATURE

A	[m ²]	cross sectional area	c	[m]	chord length
\dot{m}	[kg/s]	mass flow rate	c_0	[m]	mean chamber line length
P_{avail}	[W]	available fluid power	R	[m]	turbine radius
P_{max}	[W]	maximum power	H	[m]	turbine height
P_{limit}	[W]	power of effective limit	x_s^*	[-]	nondimensionalized axial coordinate
V	[m/s]	fluid velocity	y_s^*	[-]	nondimensionalized radial coordinate
V_i	[m/s]	fluid upstream velocity	θ	[⁰]	azimuthal angle
V_0	[m/s]	fluid downstream velocity	ρ	[kg/m ³]	fluid density

1. INTRODUCTION

New and renewable energy sources are important in order to guarantee a sustainable power production in the future. Ocean energy is one of the largest unexploited renewable energy sources on our planet. Preliminary surveys show that marine current power has a potential to supply a significant part of the future European energy needs [1]. In Sweden there are no tidal or ocean currents but many rivers and some narrow straits where the water streams are fast enough. However, the principles for the energy conversion are the same.

Recent development in offshore industry and wind power technology, which also can be applied to new energy sources, has made energy extraction from ocean and tidal marine currents a realistic alternative. An important advantage of ocean and tidal currents is that they give a highly predictable power output unlike some other renewable energy sources for example wind or solar energy. Apart from that, energy extraction from unregulated watercourses has very much in common with wind power, the main difference being the

density of the water, which is approximately 800 times the density of air. This means that a turbine rotor for underwater applications can be smaller than an air turbine.

Compared to other renewable power technologies there has been relatively little research on utilizing marine current energy. At present, no commercial marine current power plants have been built. However, there are a couple of prototypes under construction. For example in Hammerfest, Norway a 350 kW prototype is ready to be connected to the grid Marine Current Turbines Ltd has also recently launched a 300kW tidal current power plant.

All underwater current power plants so far make use of gearboxes to speed up the generators. This is necessary as most generators are optimized for a much higher speed than can be achieved from a marine current turbine. A so-called direct drive generator system does not include a mechanical gearbox. The low speed of a direct drive rotor means that a larger number of poles are needed in the stator to maintain the frequency. A larger number of poles mean a larger rotor diameter. The larger size increases the material costs and therefore it is crucial to find an effective design of the generator. Also, if a conventional horizontal axis turbine is used, a large generator will disturb the flow through the turbine. However, with a vertical axis turbine the generator can be placed on the bottom of the watercourse or above the surface.

2. CROSS FLOW TURBINES

Turbines in which the direction of flow is across the axis of rotation are commonly referred to as “vertical axis” turbines, since their axis is usually vertical. However they are more accurately described as “cross flow” since their distinguishing feature is the fact that the direction of flow is across the axis of rotation, which may be horizontal.

Recently a 6 m diameter vertical axis turbine has been installed in the Strait of Messina, between Sicily and the Italian mainland. It is expected to produce about 50 kW electrical in a 2.4 m/s current [3]. Gorlov and co-workers in the United States have tested models of a cross-flow turbine with helical blades and claim that its performance is superior to a conventional Darrieus cross flow turbine [4]. Gorlov has proposed large helical blade turbines to convert energy from the Gulf Stream. Salter [5] has proposed a large cross-flow turbine with 10 blades supported by rings top and bottom, driving ring-cam hydraulic pumps to deliver 10 MW in a 4 m/s current.

The less well-known method of extracting energy from tidal and other flows is to convert the kinetic energy of moving water directly to mechanical shaft power without otherwise interrupting the natural flow, in a manner analogous to a wind turbine. This concept is not entirely new, having been investigated by Reading University in the UK in 1979 [6], by Davis in Canada [2] and by Hilton in Australia at about the same time [7].

However direct conversion has several advantages:

- The capital cost of civil works is eliminated.
- Disruption to ecosystems and boating is minimised.
- Ocean currents, wind-induced currents and river flows as well as tidal flows can be used. There is no need for a large tidal rise and fall – for example the Messina strait between Sicily and the Italian mainland has 2.4 m/s currents with negligible rise and fall [2]. Hence a wider range of sites can be exploited, including rivers, straits between islands, sites off headlands and any other sites where there is frequent or constant strong flow.

There are also some potential problems with tidal or marine current turbines. These include:

1. Very large downstream drag forces, several times larger than those acting on a wind turbine of similar power output, requiring strong anchorage.
2. Weed growth on blades, which could reduce their efficiency.
3. Corrosion.
4. Storm damage.
5. Possible danger to shipping and to swimmers in some areas.

3. OPEN TURBINES OPERATION

Practically all hydraulic turbines that are presently used for hydropower generation have been developed for installation in water dams across streams. This conventional design is the most economical and energy efficient for river hydropower plants because it provides maximum water heads and forces all the water to flow through the turbines under maximum hydraulic pressure. However, dams damage the environment and interfere with fish migration.

They also cannot be used for power systems extracting energy from such huge potential sources as ocean currents or low-grade rivers. Thus, new hydraulic turbines are needed that can operate efficiently in free flow without dams. For decades scientists and engineers have tried unsuccessfully to utilize conventional turbines for free and low-head hydro. The very efficient hydraulic turbines in high heads become so expensive in applications for low and ultralow-head hydroelectric stations that only very modest developments of this kind are found in practice. For example, the unit cost of the Kaplan turbine jumps by a factor of 4 when the water head falls from 2–5 m.

The principal difference between exploiting high-head and free flow turbines is that the latter need large flow openings to capture as much water masses as possible with low velocities and pressure. Conventional turbines, in contrast, are designed for high pressure and relatively small water ducts where all water has no chance to escape the turbine installed in the dam body. According to the Bernoulli theorem, the density of potential energy of flow is proportional to the pressure, while the density of the kinetic energy is proportional to the square of velocity. Conventional water turbines utilize mostly the potential component at the expense of the kinetic one. In order to do so, they need so-called “high solidity” where turbine blades cover most of the inside flow passage, resisting water flow and building up the water head. This causes the fluid velocity to fall and the kinetic component of Bernoulli equation to become negligibly small compared to the potential component. That is the reason why the higher water heads correspond to higher efficiency of hydraulic turbines, an efficiency that comes close to 90 percent in some cases. However, the situation is completely reversed for free water flows. In this case, the kinetic part dominates, and conventional turbines perform poorly, becoming very expensive.

Open turbines extract energy from the fluid by reducing the flow velocity with little or no pressure reduction as the fluid passes through the turbine rotor. The streamlines must therefore expand to maintain continuity and they cannot expand indefinitely: hence there is a theoretical limit to the percentage of kinetic energy that can be extracted from the fluid. This limit has been shown by Betz [8] to be $16/27$ or 59.3% for a single actuator disk (i.e. surface across which energy is extracted as the flow passes through it) (Figure 1).

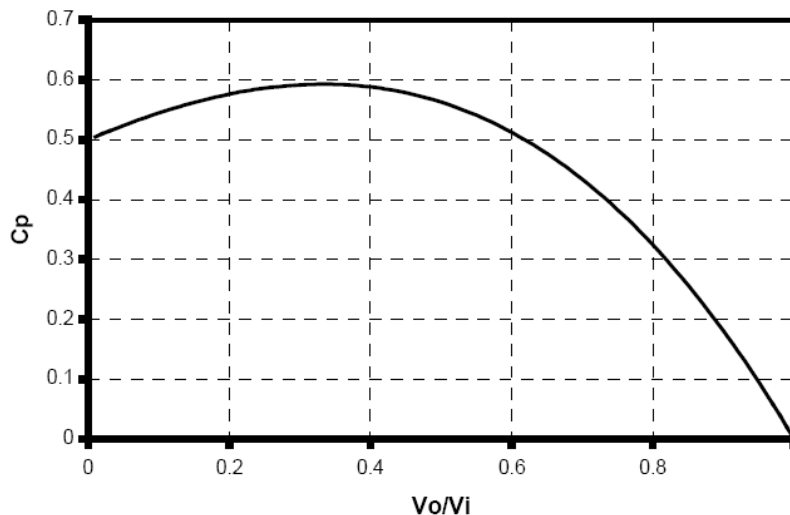


Figure 1. Power coefficient (C_p) versus upstream and downstream velocity ratios.

3.1. Energy from the water

In physics it can be shown that

$$KE = \frac{1}{2} m \cdot v^2, \quad (1)$$

and, in fluid dynamics, given a *mass flow rate* (\dot{m}) of air with density (ρ) through a surface of area (A), the available fluid power becomes

$$P_{avail} = \frac{1}{2} \dot{m} \cdot v^2, \quad (2)$$

or,

$$P_{avail} = \frac{1}{2} \rho \cdot A \cdot v^3, \quad (3)$$

where $\dot{m} = \rho \cdot A \cdot v$ [kg/s], ρ = density[kg / m^3], A =cross sectional area[m^2], v =fluid velocity[m/s].

The equations above characterize the dynamic power is available in any fluid. Therefore, they also describe the water power incident a turbine with a *rotor swept area* (A_r) and a given water density and water speed. While this calculation does provide a baseline for comparing two competing sites for installing a turbine or building a farm, it is more useful to determine the power *captured* by the turbine. This value is a function of the difference between the upstream (V_i) and downstream (V_0) water velocities, and is given by

$$P_0 = \frac{1}{2} \dot{m}(V_i^2 - V_0^2), \quad (4)$$

Moreover, assuming fluid velocity is discontinuous at the turbine's vertical plane, the mass flow rate through the turbine can be approximated as

$$\dot{m} = \rho \cdot A_r \cdot \left(\frac{V_i + V_0}{2} \right), \quad (5)$$

and, substitution yields an equation for the maximum power that can be extracted from the fluid in terms of upstream fluid velocity alone.

$$P_{max} = \frac{1}{2} C_p \cdot \rho \cdot A_r \cdot V_i^3, \quad (6)$$

The constant C_p is the *power coefficient* shown in Figure 1 above. The value C_p depends on the ratio of downstream to upstream fluid velocities (V_0/V_i) and has a theoretical maximum value of 16/27 or 0.59 according to the Betz Limit [8]. Therefore, because the most efficient, high speed, two- and three-blade turbines have a power coefficient of just less than 0.50, rotor power has an effective limit given below:

$$P_{limit} = \frac{1}{4} \rho \cdot A_r \cdot V_i^3, \quad (7)$$

4. ACHARD TURBINE DESCRIPTION

The vertical axis Achard turbine from Figure 2 consists of a runner with three vertical delta blades, sustained by radial supports at the mid-height of the turbine, and stiffened with circular rims at the upper and lower part of the turbine. The blades and their radial supports are shaped with NACA 4518 airfoils, while the circular rims are shaped with lens type airfoil.

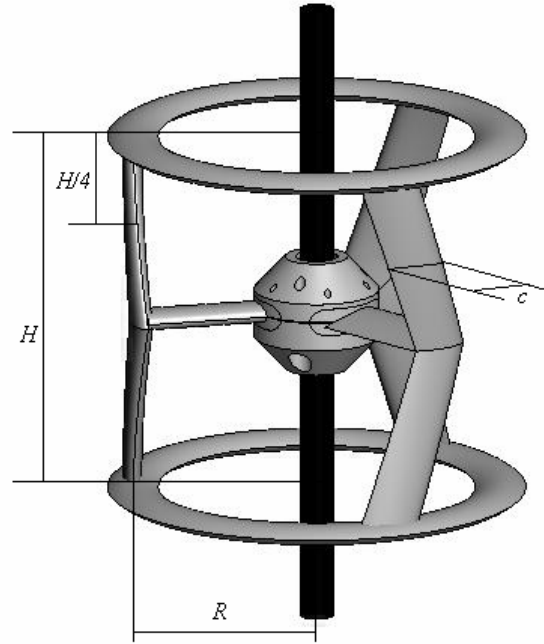


Figure 2. Achard turbine (by courtesy of LEGI).

The turbine radius is $R = 0.5$ m, and the turbine height is $H = 1$ m. In Figure 3 we present the Achard turbine geometry generated in MATLAB (the upper and lower rims are not represented here). Along each delta blade, the airfoil mean camber line length c_0 varies from 0.18 m at $z = 0$, to 0.12 m at the extremities, where $z = \pm 0.5$ m. Between the leading edge of the blade's extremity and the leading edge of the blade at mid-height of the turbine, there is a 30° azimuth angle.

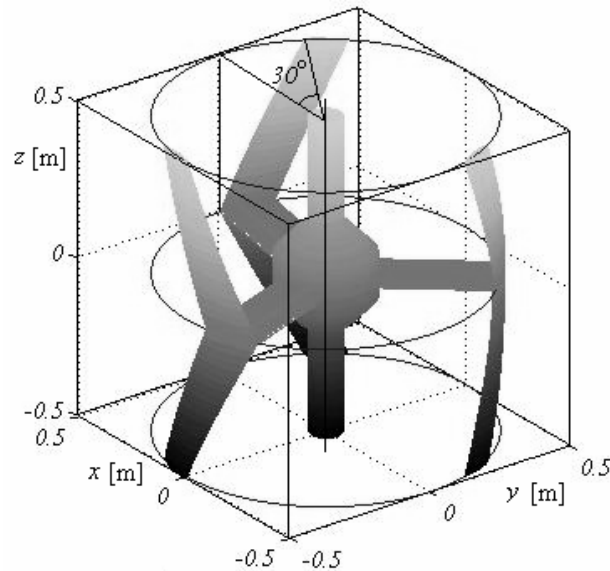


Figure 3. Achard turbine geometry.

At $z = \pm H/4 = \pm 0.25$ m, the horizontal cross-section of the runner gives airfoils with $c_0 = 0.15$ m (the mean value of the mean camber line length along the delta wing), and with the chord length $c = 0.1494$ m. Within this paper, the 2D computations correspond to the cross-plane placed at $z = 0.25$ m level (Figure

4), where the three blade profiles have a mean camber line length of $c_0 = 0.15$ m. The values of the azimuth angle of the blades in Figure 4 are $\theta = \{0^\circ; 120^\circ; 240^\circ\}$, in counter clockwise direction.

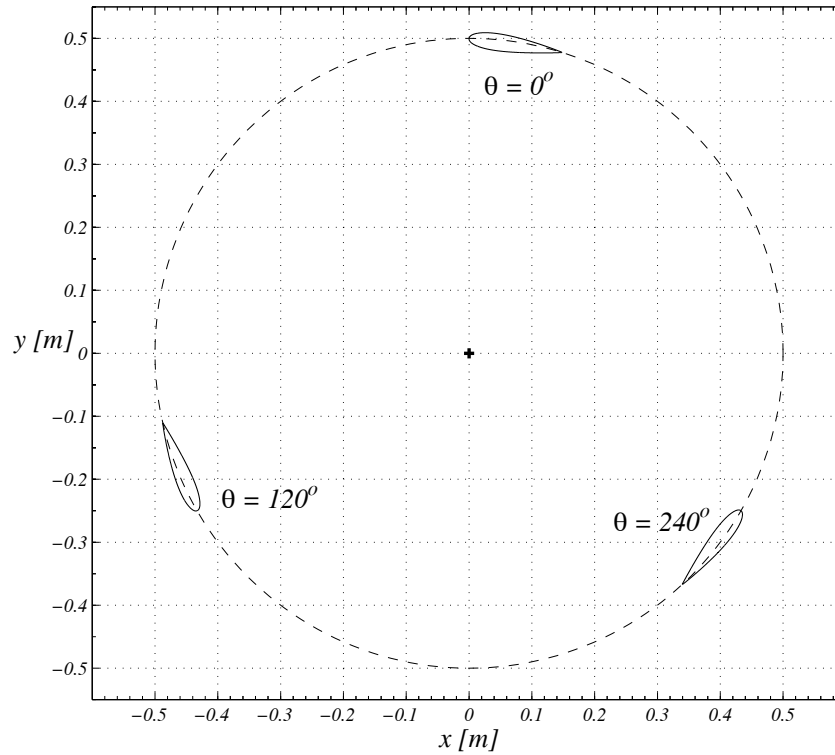


Figure 4. Computational runner cross-section.

The runner blades are shaped with NACA airfoils of four-digit series, where the first digit is the maximum upper camber m (as percentage of the chord), the second digit is the distance p of the maximum upper camber from the airfoil leading edge (in tens of percents of the chord), and the last two digits describe the maximum thickness of the airfoil, d as percent of the chord length. For the Achard turbine blades, we consider $d = 18\%$.

In a xOy plane, the airfoil coordinates $\{x, y\}$ are nondimensionalised with respect to the chord length c , with $x^* = 0$ at the leading edge and with $x^* = 1$ at the trailing edge (the dimensionless variables are denoted with an asterisk).

The dimensionless coordinates $\{x^*, y_s^*\}$ of the airfoil mean camber line are defined as:

$$y_s^* = \frac{m^*}{p^{*2}}(2p^* - 1)x^{*2} \quad \text{for} \quad 0 \leq x^* < m^* \quad (8)$$

$$y_s^* = \frac{m^*}{(1 - p^*)^2} \left[(1 - 2p^*) + 2p^*x^* - x^{*2} \right] \quad \text{for} \quad m^* \leq x^* \leq 1,$$

where $p^* = 0.5$, since the mean camber line of the airfoil is along the circle of radius $R = 0.5$ m, as in Figure 4. So, the second digit of the NACA airfoil is 5, because the maximum upper camber is placed at a half-distance between the leading edge and the trailing edge.

The coordinates $\{x^*, y_s^*\}$ of the upper and lower surfaces of the NACA airfoil are defined by:

$$y_s^* = y_s^* \pm \frac{d}{20} \left(0.29690\sqrt{x^*} - 0.12600x^* - 0.35160x^{*2} + 0.28430x^{*3} - 0.10150x^{*4} \right), \quad (9)$$

The chord length c can be expressed upon the runner radius and the mean camber line length c_0 :

$$c = 2R \sin(c_0/2R), \quad (10)$$

For $R = 0.5$ m and $c_0 = 0.15$ m, we obtain the mean chord length $c = 0.1494$ m at $z = 0.25$ m.

The maximum upper camber is defined as:

$$m = R(1 - \cos(c_0/2R)). \quad (11)$$

Its dimensionless value is $m^* = m/c = 0.03758$. As percentage of the chord, $m = 3.758\% \cong 4\%$, so the first digit of the NACA airfoil is 4.

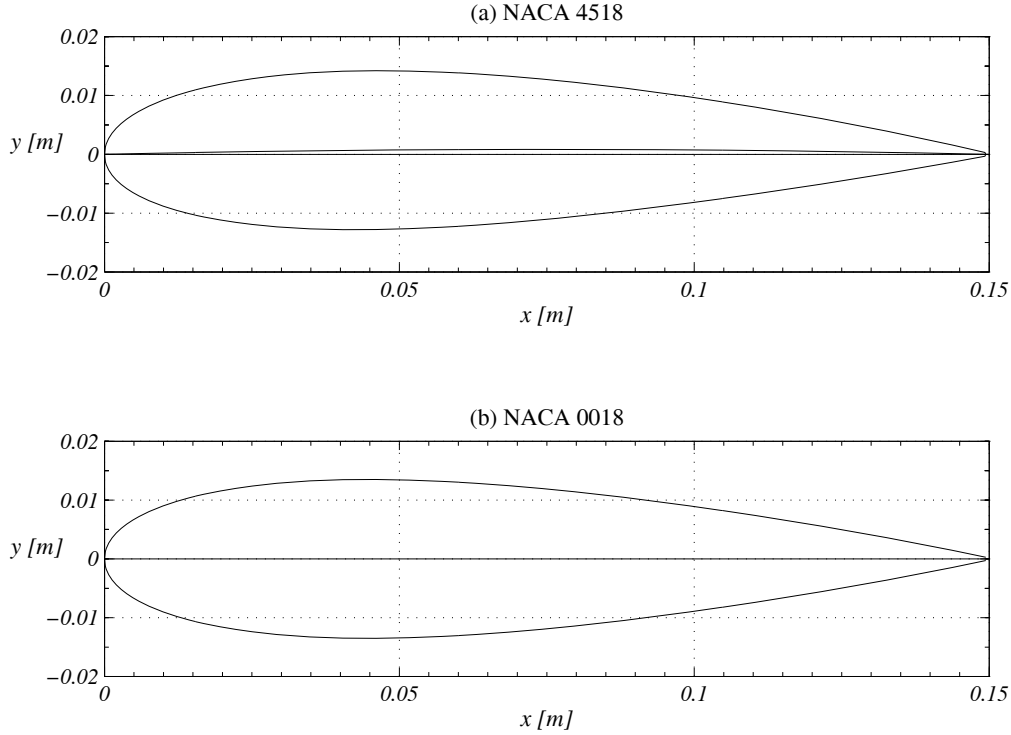


Figure 5. Blade profiles for $c_0 = 0.15$ m: (a) curved airfoil NACA 4518; (b) straight airfoil NACA 0018.

Thus, the airfoil type corresponding to the Achard turbine blades is NACA 4518, an airfoil with the mean camber line along the runner circumference (Figure 5a). The computations from section 4, are performed for the profile NACA 4518 and also for the straight profile NACA 0018, which can be generated from (Eq. 9) for $y_s^* = 0$, since $m^* = 0$ in (Eq. 8). For the NACA 0018 airfoil, the chord length is $c = c_0 = 0.15$ m (Figure 5b). That last choice is due to the fact that experimental and numerical data are available for such a straight profile, corresponding to a Darrieus marine turbine, a vertical axis cross-flow turbine with two straight blades of 0.15 m chord length [11, 12].

5. NUMERICAL APPROACH

To simulate the fluid flow the numerical code FLUENT [9] was used. The code uses a control-volume-based technique to convert the governing equations in algebraic equations that can be solved numerically. This control volume technique consists of integrating the governing equations at each control volume, yielding discrete equations that conserve each quantity on a control-volume basis. The governing integral equations for the conservation of mass and momentum, and (when appropriate) for energy and other scalars, such as turbulence and chemical species, are solved sequentially. Being the governing equations non-linear (and coupled), several iterations of the solution loop must be performed before a converged solution is

obtained. The flow solution procedure is the SIMPLE routine [9]. This solution method is designed for incompressible flows, thus being implicit. The full Navier-Stokes equations are solved. The flow was assumed to be steady, and isothermal. In these calculations turbulence effects were considered using turbulence models, as the $k-\varepsilon$ RNG models, with the modification of the turbulent viscosity. To model the flow close to the wall, standard wall-function approach was used, and then the enhanced wall functions approach has been used to model the near-wall region (i.e., laminar sub layer, buffer region, and fully-turbulent outer region). For this model, the used numerical scheme of the flow equations was the segregated implicit solver. For the model discretization, the SIMPLE scheme was employed for pressure-velocity coupling, second-order upwind for the momentum equations, and first-order up-wind for other transport equations (e.g. vapor transport and turbulence modeling equations). Computational domain is discretized using the GAMBIT preprocessor [9]. The flow close to the body surface is of particular importance in the current study, the mesh structure in the computational domain deliberately reflects this concern by heavily clustering the mesh close to the solid surface of the body so that the boundary layer mesh is used encloses the body surface.

6. RESULTS AND DISCUSSION

An enlarged view of the mesh showing the hydrofoil for different azimuth angle is shown in Figures 6, 8 and 10. It can be observed that the node density is high near the hydrofoil, especially near the leading and trailing edges. This is necessary since the gradients are very high in this region of the flow field.

The following are the results obtained from the Fluent solver used to determine the velocity and pressure fields.

- Pressure contours. Figure 7a shows the pressure contours in the flow field. Since, the angle of attack is zero the pressure distribution is symmetrical about the hydrofoil centerline.
- Velocity distribution. Figure 6b shows the velocity vectors in the flow around the hydrofoil. It can be seen that the flow is streamlined and the maximum velocity zone corresponds to the minimum pressure zone in Figure 7a.
- Pressure distribution along the hydrofoil surface. Figure 7b shows the distribution of static pressure along the surface of the hydrofoil. The leading edge of the hydrofoil experiences very high pressure. The static pressure drops rapidly as we move along the surface corresponding to increasing flow velocity. After the minimum pressure point, the static pressure begins to rise.

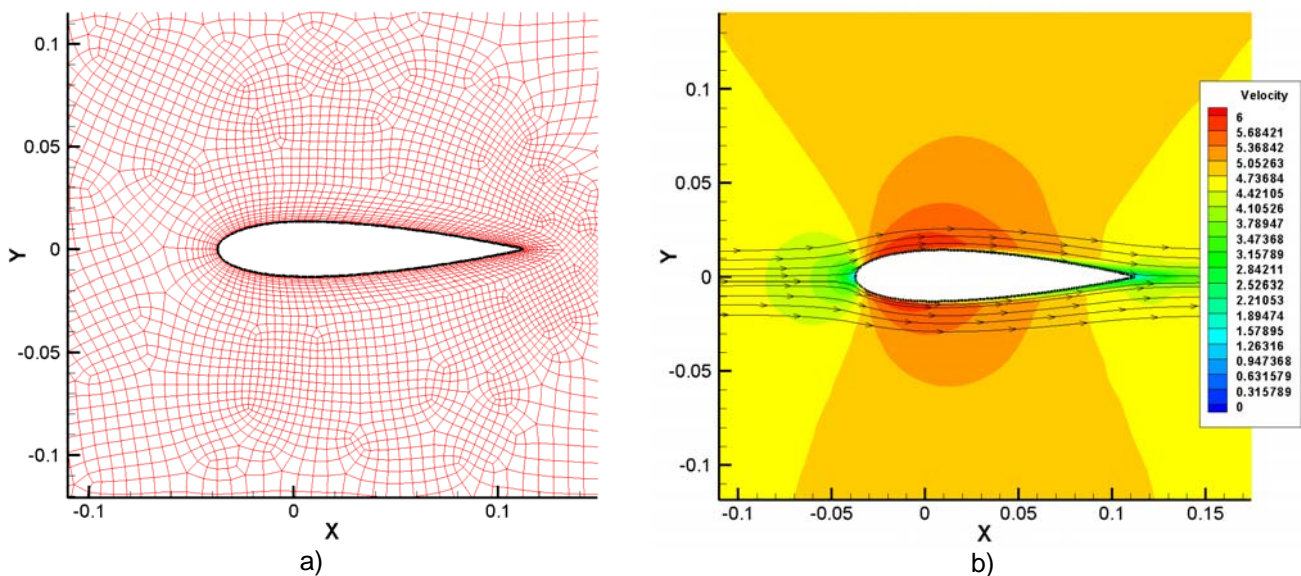


Figure 6. Enlarged view of the mesh showing the hydrofoil (a); Velocity field (colored by velocity magnitude in m/s) and selected streamlines (b), around the blade for the azimuth angle $\theta = 0^\circ$.

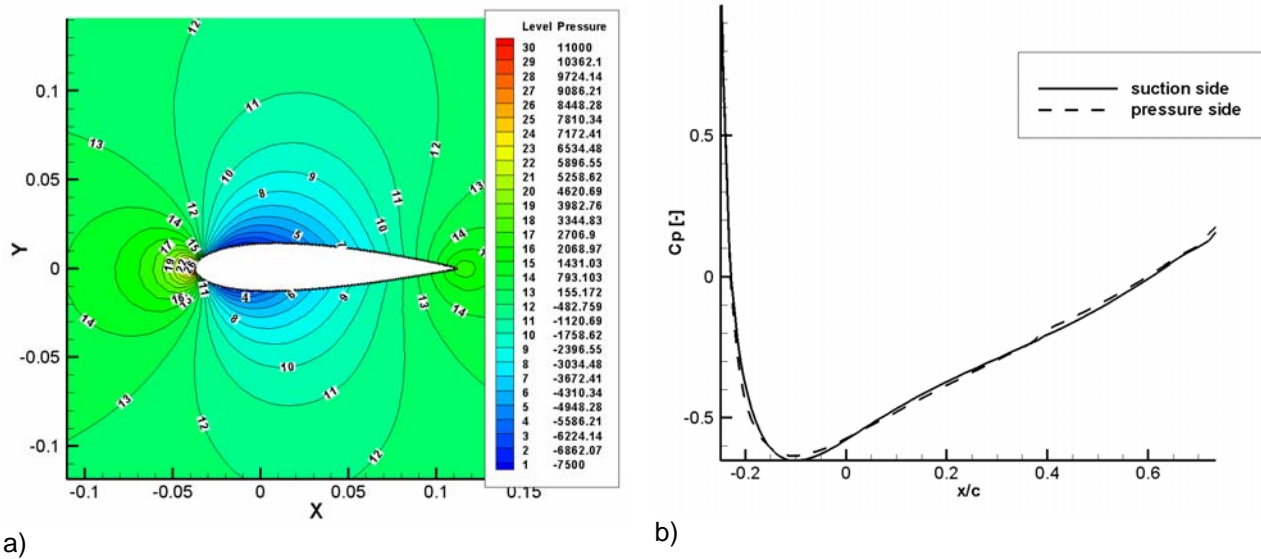


Figure 7. Static pressure contours around the hydrofoil (in Pa) (a); static pressure distribution along the hydrofoil surface (b) around the blade for the azimuth angle $\theta = 0^\circ$.

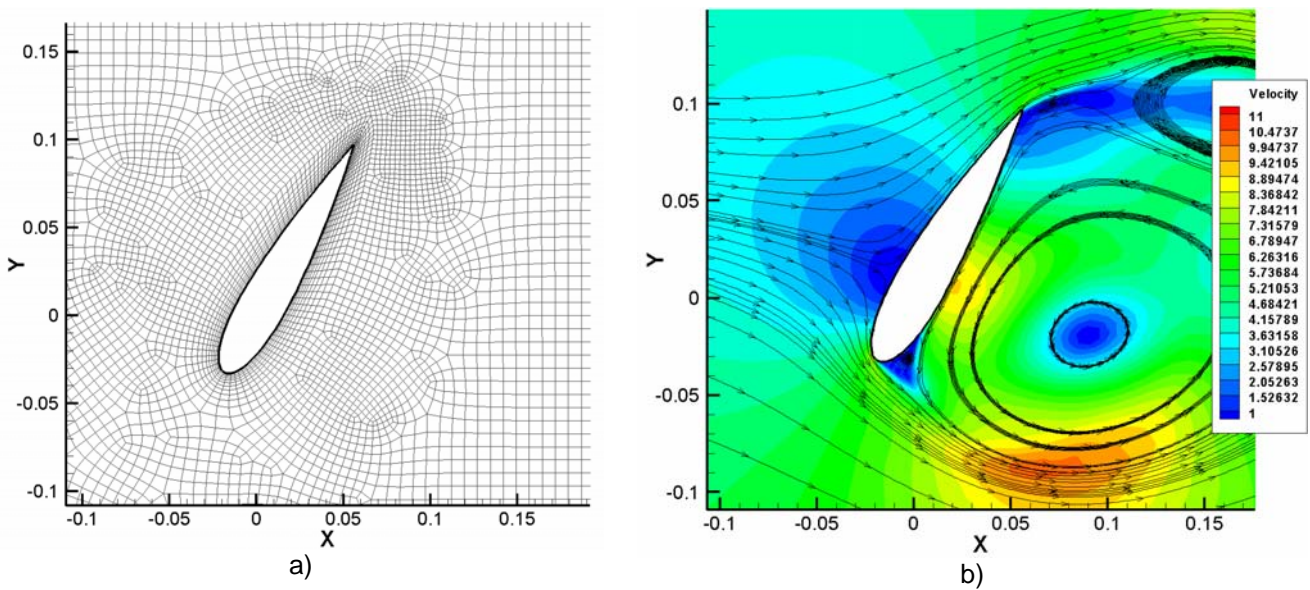


Figure 8. Enlarged view of the mesh showing the hydrofoil (a); Velocity field (colored by velocity magnitude in m/s) and selected streamlines (b), around the blade for the azimuth angle $\theta = 60^\circ$.

The pressure distribution results (Fig. 9a) show that a perturbed high impulse constantly arises and stays at the bottom of the hydrofoil that makes unsteady flow produce the periodical vortex shedding. Consequently, the periodic low-pressure zone is released along the hydrofoil surface by this shedding.

The flow separation of the foil generate the vortex shedding there and therefore cavitation is can produced in this region.

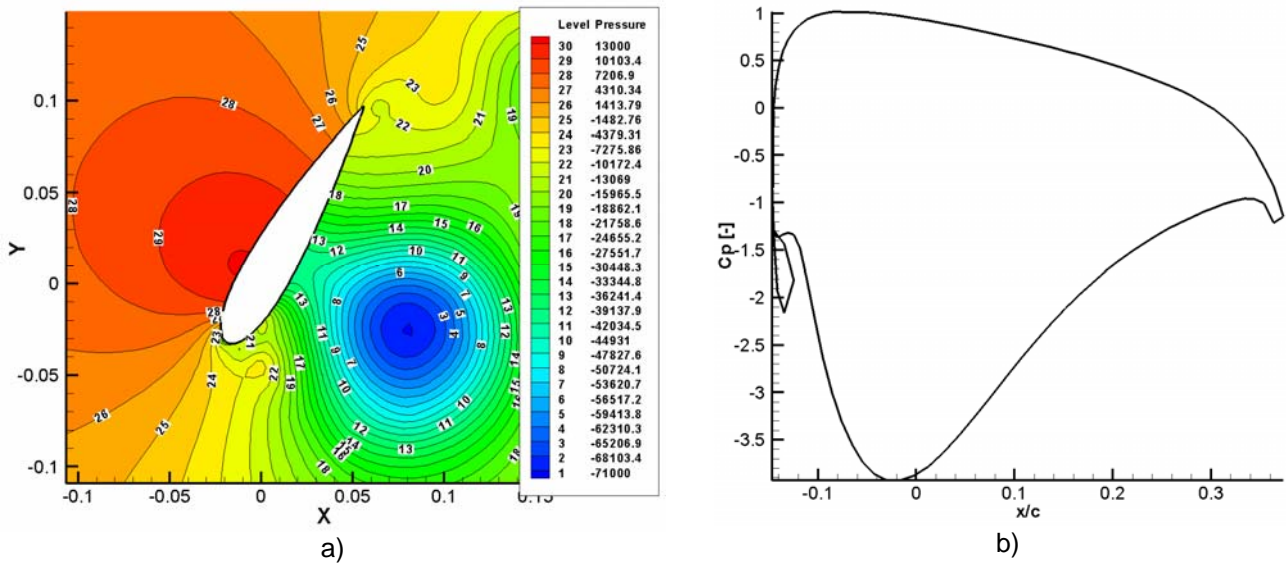


Figure 9. Static pressure contours around the hydrofoil (in Pa) (a); static pressure distribution along the hydrofoil surface (b) around the blade for the azimuth angle $\theta = 60^\circ$.

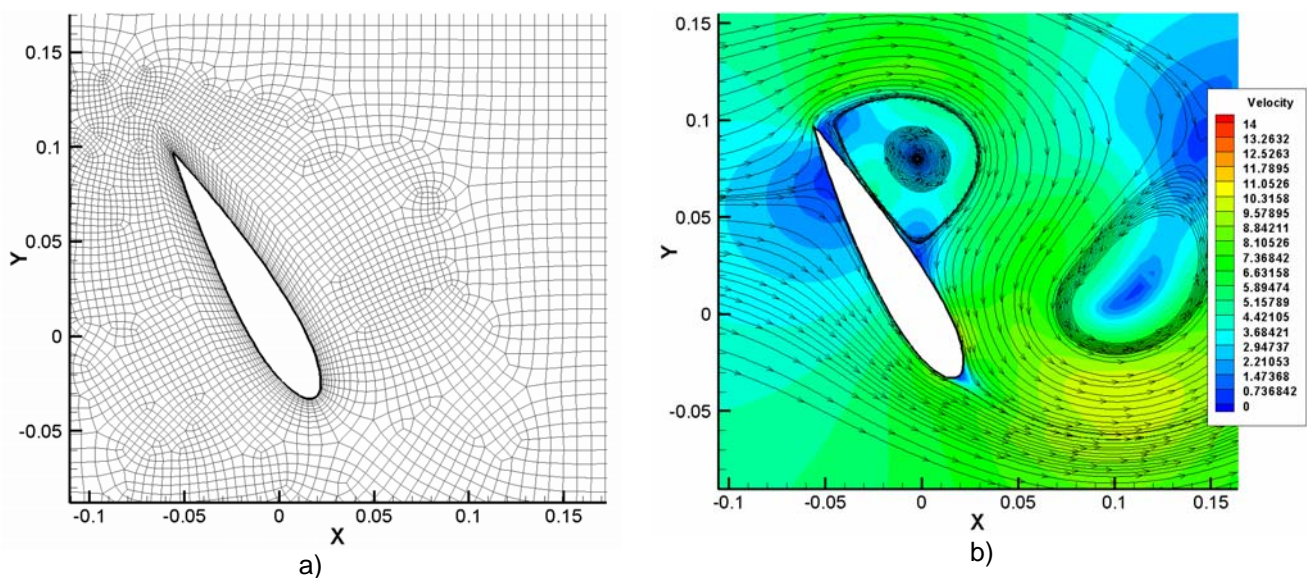


Figure 10. Enlarged view of the mesh showing the hydrofoil (a); Velocity field (colored by velocity magnitude in m/s) and selected streamlines (b), around the blade for the azimuth angle $\theta = 120^\circ$.

Fig. 10b and 11 shows the velocity and pressure structures around the foil for the azimuth angle $\theta = 120^\circ$. From the pressure field result, we see that, although there still exists flow separation, pressure perturbation does not occur (Fig. 11b).

Observations in the wake of the hydrofoil indicate a significant effect of the vortex shedding into the flow. This effect is so strong that fluctuations in the data rate of the numerical simulations can be used to measure the frequency of shedding. Conclusions is that the numerical simulations appear to capture much of the fundamental physics of the fluid flow around the Achard turbine blades.

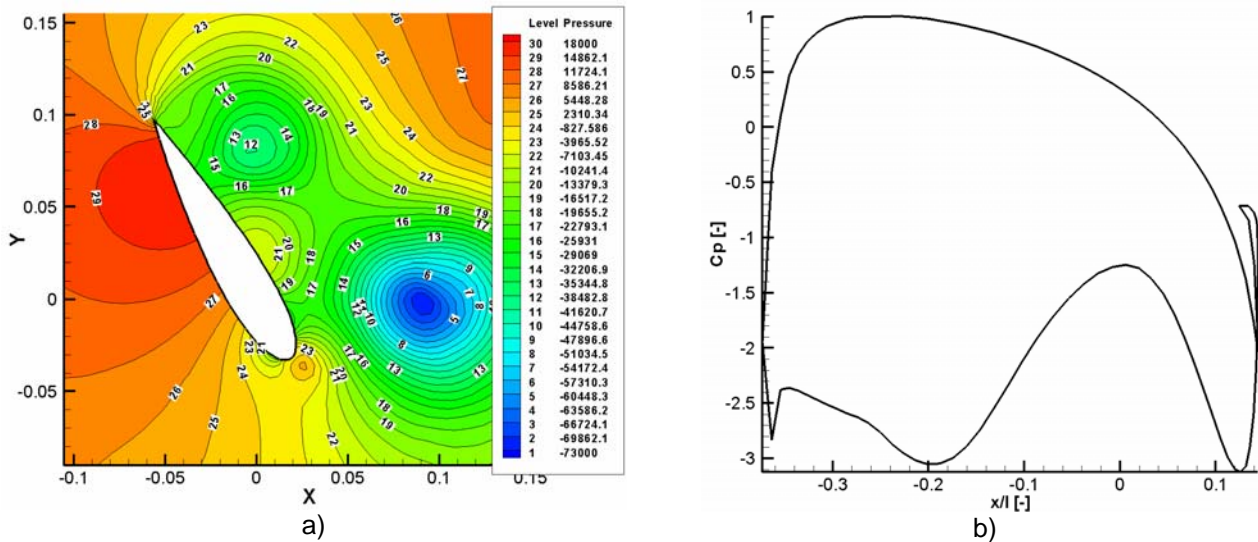


Figure 11. Static pressure contours around the hydrofoil (in Pa) (a); pressure coefficient distribution along the hydrofoil surface (b) around the blade for the azimuth angle $\theta = 120^\circ$.

7. CONCLUSIONS

Water current turbines, which operate in a manner analogous to a wind turbine, are a relatively new technology which can generate power from flowing water with very little environmental impact.

It can be shown that maximum power which can be extracted from the flow is 59% as the fluid must have sufficient kinetic energy to leave the power extraction region. This is known as the Betz criterion and applies to all free stream turbines whether operating in air or water. It applies to shrouded turbines both vertical and horizontal axis and oscillating hydrofoils.

The model of a free-flow turbine reveals a new class of problems about streamlining with partial penetrating through an obstacle; some of these problems could admit explicit solutions and could have other applications.

In this paper, 2D numerical computations are performed with Fluent 6.3 software, in order to depict the steady flow around a cross-section of a blade of the Achard turbine. The value of the upstream velocity is taken so that the Reynolds number on the fixed profile exceeds 10^5 , thus the flow may be assumed to have the same characteristics as in the real rotating case.

In the real case the turbine rotation speed is restricted by the phenomenon of cavitation. It occurs when the partial pressure of the water locally falls below the vapor pressure of the water and it can cause serious damage to the turbine blades. Cavitation happens when the turbine blade moves too fast through the water, therefore the turbine speed has to be restricted. The maximum speed of the turbine blades relative to the water occurs at the point where the turbine moves opposite the direction of the flowing water. Thus the turbine diameter and the flow velocity restrict the turbine rotation speed. A large turbine radius and a high water flow velocity imply a low rotation speed and vice versa.

The next step is focus on the numerical analysis of the cavitating flows around the Achard turbine blades.

ACKNOWLEDGMENTS

This work has been supported by Romanian National Authority for Scientific Research, Research of Excellence Programme CEEEX, grant no: 192/2006, CEEEX-THARVEST. Special thanks are addressed to Dr. Jean-Luc Achard, CNRS Research Director, and to PhD student Ervin Amet from LEGI Grenoble, France, for consultancy and documentation on the Achard turbine.

REFERENCES

1. BAKER, A.C. *Tidal Power*. Peter Peregrinus Ltd, 1991.
2. Blue Energy Canada. <http://www.blueenergy.com>. Accessed 6 March 1999, 30 Sept 2002.
3. COIRO, D. Dept of Aeronautical Eng, University of Naples. *Pers. Comm*, 2001, 2003.
4. GORBAN, A.N., GORLOV, A.M. and SILANTYEV, V.M. *Limits of the turbine efficiency for free fluid flow*. J. Energy Res. Technology, Vol. **123**, pp: 311-317, 2001.
5. SALTER, S.H. *Proposal for a large, vertical-axis tidal-stream generator with ring-cam hydraulics*. Proc 3rd European Wave Energy Conf, Patras, Greece, 30 Sept-2 Oct, 1998. <http://www.mech.ed.ac.uk/research/wavepower>.
6. GARMAN, P. *Water current turbines: a fieldworker's guide*. IT Publications, London, 1986.
7. HILTON, D.J. *A vertical axis water turbine for extracting energy from rivers and tidal currents*. Proc. 1st Internat Conf on Technology for Development, IE Aust/ADAB et al, Canberra, 24-28 Nov. 1980, pp:138-141.
8. BETZ, A. *Das Maximum der theoretisch möglichen Ausnützung des Windes durch Windmotoren*. Zeitschrift für das gesamte Turbinenwesen, Heft 26, Sept.26, 1920.
9. FLUENT 6.3 User's Guide, Fluent Incorporated, Lebanon, USA.
10. PLOESTEANU C. *Étude hydro-dynamique d'une type d'hydraulienne à axe vertical pour les courants marins*. Thèse de Doctorat Institut National Polytechnique de Grenoble, France, 2004.
11. MAÎTRE T., ACHARD J-L., GUITTET L., PLOEȘTEANU C., *Marine turbine development: Numerical and experimental investigations*. Sci. Bull. of the Politehnica University of Timisoara, Transactions on Mechanics, vol **50 (64)**, 2005, pp: 59-66.
12. AMET E., PELLONE C., MAÎTRE T., *A numerical approach for estimating the aerodynamic characteristics of a two bladed vertical Darrieus wind turbine*, Scientific Bulletin of the Politehnica University of Timisoara, Transactions on Mechanics, vol **51 (65)**, 2006, pp: 95-102.
13. SHIONO M., SUZUKI K., KIHIO S., *Output characteristics of Darrieus water turbine with helical blades for tidal current generations*, Proceedings of the Twelfth International Offshore and Polar Engineering Conference, Kitakyushu, Japan, May 26-31, 2002.
14. ACHARD J.-L., MAÎTRE T., *Turbomachine hydraulique*. Brevet déposé, Code FR 04 50209, Titulaire: Institut National Polytechnique de Grenoble, 2004.
15. Gorlov A. *Helical turbine for the Gulf Stream: Conceptual Approach to Design of a Large-Scale Floating Power Farm*, Marine Technologie, Vol. **35**, No. 3, pp: 175-182, 1998.
16. PARASCHIVOIU, I., DELCLAUX, F., FRAUNIE, P., BÉGUIER, C., *Aerodynamic Analysis of the Darrieus Rotor Including Secondary Effects*, Journal of Energy, Vol. **7**, No. 5, pp: 416-422, 1983.
17. SHIONO M., SUZUKI K., KIHIO S., *An experimental study of the characteristics of a Darrieus turbine for tidal power generation*, Electrical Engineering in Japan, Vol. **132**, No. 3, pp: 38-47, 2000.

Received, May12, 2008